International Journal for Parasitology: Drugs and Drug Resistance 22 (2023) 9–19

Contents lists available at ScienceDirect

International Journal for Parasitology: Drugs and Drug Resistance

journal homepage: www.elsevier.com/locate/ijpddr

Transcriptomic analysis of albendazole resistance in human diarrheal parasite *Giardia duodenalis*

Qiao Su [a,c], Louise Baker [a,b], Samantha Emery [a], Balu Balan [a], Brendan Ansell [a], Swapnil Tichkule [a], Ivo Mueller [a,c,d], Staffan G. Svärd [e], Aaron Jex [a,b,c,*]

[a] Population Health and Immunity Division, The Walter and Eliza Hall Institute of Medical Research, Melbourne, VIC, Australia
[b] Department of Veterinary Biosciences, Melbourne Veterinary School, Faculty of Veterinary and Agricultural Sciences, The University of Melbourne, Parkville, VIC, Australia
[c] Department of Medical Biology, The University of Melbourne, Parkville, VIC, Australia
[d] Unité Malaria: Parasites et Hôtes, Département Parasites et Insectes Vecteurs, Institut Pasteur, F-75015, Paris, France
[e] Department of Cell and Molecular Biology, BMC, Uppsala University, Uppsala, Sweden

ARTICLE INFO

Keywords:
Giardia duodenalis
Albendazole
Drug-resistance

ABSTRACT

Benzimidazole-2-carbamates (BZ, e.g., albendazole; ALB), which bind β-tubulin to disrupt microtubule polymerization, are one of two primary compound classes used to treat giardiasis. In most parasitic nematodes and fungi, BZ-resistance is caused by β-tubulin mutations and its molecular mode of action (MOA) is well studied. In contrast, in *Giardia duodenalis* BZ MOA or resistance is less well understood, may involve target-specific and broader impacts including cellular damage and oxidative stress, and its underlying cause is not clearly determined. Previously, we identified acquisition of a single nucleotide polymorphism, E198K, in β-tubulin in ALB-resistant (ALB-R) *G. duodenalis* WB-1B relative to ALB-sensitive (ALB-S) parental controls. E198K is linked to BZ-resistance in fungi and its allelic frequency correlated with the magnitude of BZ-resistance in *G. duodenalis* WB-1B. Here, we undertook detailed transcriptomic comparisons of these ALB-S and ALB-R *G. duodenalis* WB-1B cultures. The primary transcriptional changes with ALB-R in *G. duodenalis* WB-1B indicated increased protein degradation and turnover, and up-regulation of tubulin, and related genes, associated with the adhesive disc and basal bodies. These findings are consistent with previous observations noting focused disintegration of the disc and associated structures in *Giardia duodenalis* upon ALB exposure. We also saw transcriptional changes with ALB-R in *G. duodenalis* WB-1B consistent with prior observations of a shift from glycolysis to arginine metabolism for ATP production and possible changes to aspects of the vesicular trafficking system that require further investigation. Finally, we saw mixed transcriptional changes associated with DNA repair and oxidative stress responses in the *G. duodenalis* WB-1B line. These changes may be indicative of a role for H_2O_2 degradation in ALB-R, as has been observed in other *G. duodenalis* cell cultures. However, they were below the transcriptional fold-change threshold ($\log_2FC > 1$) typically employed in transcriptomic analyses and appear to be contradicted in ALB-R *G. duodenalis* WB-1B by down-regulation of the NAD scavenging and conversion pathways required to support these stress pathways and up-regulation of many highly oxidation sensitive iron-sulphur (FeS) cluster based metabolic enzymes.

1. Introduction

Giardia duodenalis is a gastrointestinal parasite causing ~1 billion infections and ~280 million symptomatic cases (Giardiasis) each year (Lane and Lloyd, 2002), making it the fourth most common cause of foodborne illness worldwide (Torgerson et al., 2015). Resilient *G. duodenalis* cysts and their zoonotic/anthroponotic transmission through food, water, or direct contact make *Giardia* a common parasite

Abbreviations: BZ, benzimidazole; MTZ, metronidazole; ALB, albendazole; MOA, mode of action; ALB-R, albendazole resistant line; ALB-S, albendazole susceptible line; TUB1, β-tubulin isoform 1; CBS, colchicine binding site; $\log_2$-FC, $\log_2$ fold change; TMM, Trimmed Mean of M-values; SNP, Single nucleotide polymorphisms; VSP, variant-specific surface proteins; HCMP, high cysteine membrane proteins.

* Corresponding author. Population Health and Immunity Division, The Walter and Eliza Hall Institute of Medical Research, Melbourne, VIC, Australia.
E-mail address: jex.a@wehi.edu.au (A. Jex).

https://doi.org/10.1016/j.ijpddr.2023.03.004
Received 8 November 2022; Received in revised form 9 March 2023; Accepted 21 March 2023
Available online 24 March 2023

in most countries, irrespective of socioeconomic wealth (Furness et al., 2000). Giardiasis is a significant contributor to the global diarrhoeal disease burden, a major cause of malabsorption syndrome and failure to thrive (Robertson et al., 2010), and is associated with post-infectious gastrointestinal disorders, including irritable bowel syndrome and chronic enteropathy (Guerrant et al., 2013). Treatment of giardiasis is limited to nitroheterocyclic drugs (e.g., metronidazole; MTZ) and benzimidazoles (BZs, e.g., albendazole (ALB) and mebendazole) (Escobedo and Cimerman, 2007; Solaymani-Mohammadi et al., 2010). Clinical resistance has been reported for *G. duodenalis* against each drug class and is readily generated *in vitro* (Argüello-García et al., 2020). However, although mechanisms of MTZ-resistance are well studied in *Giardia* (Ansell et al., 2015b), those underpinning BZ-resistance are less understood.

BZs bind tubulin subunits to inhibit microtubule polymerization and are broadly used to treat a range of parasites (Lacey, 1988). BZs are well tolerated and safe for children, low cost, and often effective with one or a few doses. However, BZ-resistance is widespread in many multicellular parasites, of growing concern in treating human helminthiases (James et al., 2009), and is a potential risk for controlling gastrointestinal protists, including *G. duodenalis* (Leitsch, 2015; Furtado et al., 2016). In nematodes and fungi, BZ-resistance appears primarily caused by coding mutations in β-tubulin isoform 1 (TUB1), most notably at F167, E198, and F200 (Lubega and Prichard, 1991; Yarden and Katan, 1993; Elard and Humbert, 1999; Ghisi et al., 2007; Banno et al., 2008; Rufener et al., 2009; Beech et al., 2011; Cai et al., 2015; Liu et al., 2019). These mutations disrupt the binding of BZs (specifically ALB and mebendazole) in the colchicine binding site (CBS) formed between the α- and β-tubulin interface during microtubule polymerization (Lacey, 1988; Keeling and Doolittle, 1996; Chatterji et al., 2011; Wang et al., 2016). In nematodes and fungi, BZs likely kill by inhibiting the microtubule network of transport vesicles required for glucose uptake (Allen Paris and Gottlieb, 1970; Lacey, 1988; Khan et al., 2019), leading to starvation (Jasra et al., 1990) although these drugs also induce more systemic effects (Borgers et al., 1975).

BZ MOA and resistance mechanisms are less defined in single-celled parasitic eukaryotes, such as *G. duodenalis*. The cellular biology of *G. duodenalis* is heavily dependent on microtubules, with the parasite having lost the myosin II gene and lacking canonical actin binding and actin-related proteins (Morrison et al., 2007; Steele-Ogus Melissa et al., 2021). Microtubules are critical in *Giardia's* cytoskeletal structure, adhesive disc, flagellar motor proteins, vesicular trafficking, and the cell cycle (Dawson and House, 2010; Hagen et al., 2020). In addition to having at least five tubulin isoforms (Campanati et al., 2003), *G. duodenalis* encodes a novel family of annexin-like proteins, the alpha-giardins (Weiland et al., 2005), that associate with tubulin in microtubules (Vahrmann et al., 2008). *G. duodenalis* has also undergone a significant expansion of the NEK kinases (Manning et al., 2011), which regulate tubulin polymerization across the Eukaryota (Westermann and Weber, 2003). BZs have major impacts in *G. duodenalis* on cell morphology and structure (Chavez et al., 1992), particularly leading to morphological defects and disintegration of the adhesive disc and flagella, and interruption of the cell cycle, most notably the transition from G2/M to G1 phase (Sandhu et al., 2004; Martinez-Espinosa et al., 2015). As seen with metazoans, BZs directly interact with microtubules in *Giardia* and cause a depolymerizing effect (MacDonald et al., 2004; Aguayo-Ortiz et al., 2013). BZ exposure is associated with changes in the expression of giardins, NEK kinases, and other essential players in microtubule composition and regulation in this parasite (Jiménez-Cardoso et al., 2009). Early studies of BZ-resistant *G. duodenalis* (reviewed by (Leitsch, 2015)) did not find evidence for mutations in beta-tubulin (Upcroft et al., 1996; Argüello-García et al., 2009). Several studies have implicated oxidative stress and metabolic changes with BZ exposure and *in vitro* selected resistance in *Giardia* (Paz-Maldonado et al., 2013; Argüello-Garcia et al., 2015; Pech-Santiago et al., 2022) and other organisms (Locatelli et al., 2004; Martinez-Espinosa et al., 2015; Wen et al., 2020; Kim et al., 2021; Xu et al., 2022). In addition, *in vitro* cultured *G. duodenalis* isolates and clones have demonstrated variable susceptibility to BZs (Argüello--García et al., 2004) and may indicate multiple, independent, molecular mechanisms could lead to BZ-resistance (Argüello-García et al., 2009).

In a recent analysis of *in vitro* selected ALB-resistant line (ALB-R) of the *G. duodenalis* WB-1B isolate (Emery-Corbin et al., 2021b), we identified a substitution in codon position 198 of TUB1 (GL_136020), leading to a mutation from arginine (E) to lysine (K). This E198K mutation was only identified using sensitive amplicon sequencing, and, its allelic frequency in culture correlated with the level of ALB tolerance during *in vitro* selection. This mutation has been described as causing ALB-R in fungi (Banno et al., 2008; Cai et al., 2015) and in this work, we predicted that the E198K mutation reduced the accessibility of the colchicine-binding site (CBS) of TUB1 in *G. duodenalis*. This prediction was further supported by observations of cross-resistance with BZ analogs consistent with a reshaped CBS (Emery-Corbin et al., 2021b). Here, we employ strand-specific RNA-sequencing to characterize transcriptomic changes associated with ALB-R in this same culture lineage, comparing isogenic ALB-S and ALB-R states. We examine how functional trends in these data may inform on ALB MOA and mechanisms of resistance and compare the results with prior studies on ALB-R in *G. duodenalis*.

2. Materials and methods

2.1. Axenic in vitro culture of G. duodenalis and selection for ALB-R

All *G. duodenalis* WB subclone 1B (WB–1B) (Capon et al., 1989) trophozoites were grown at 37 °C in flat-sided 10 mL tubes (Thermo Fisher Nunc Delta #156758) filled with 10 mL of complete TYI-S33 media (Keister, 1983; Davids and Gillin, 2011) containing 10% heat-inactivated bovine serum (Invitrogen #16170–078) and reduced 6 mM glucose (Ansell et al., 2017), and sub-cultured twice weekly. ALB-R was selected as per (Emery-Corbin et al., 2021b) by continuously exposing *G. duodenalis* trophozoites to ALB (Sigma Aldrich CAS 54965-21-8; 1 mM stock in dimethyl sulfoxide, DMSO, Cell Signaling #12611P) under sublethal concentration, starting at half the IC50 of ALB susceptible line (ALB-S) at 0.1 μM (Upcroft et al., 1996), followed by incremental increases of 0.01–0.05 μM over time until the cultured trophozoites were able to grow to confluence in 0.5 μM ALB (2.5x the susceptible IC50). After selection, ALB-R cultures were maintained at 0.5 μM ALB to ensure stable growth. ALB-S controls were maintained alongside the ALB-R line in complete media spiked with the equivalent DMSO vehicle.

2.2. Drug sensitivity testing

Giardia duodenalis WB-1B trophozoites from confluent tubes were detached in fresh TYI media by cooling on wet ice for 20 min and seeded into 96-well clear-bottom plate (Corning #3610) in 2000 trophozoites per well, resulting in a final 50 μL volume with ALB (2.5–20 μM) samples and 1% DMSO controls. Plates were sealed within GasPak EZ anaerobe pouches (BD #260685) with fresh anaerobic sachets and incubated at 37 °C for 48 h. 50 μL CellTiter-Glo reagent (Promega #G7571) was added to each well at room temperature (r.t.) for ATP-based luminescence screening (BioTek). Prism software (GraphPad) was used to fit Hill plots to dose-response data and to calculate IC50 values via the "log (inhibitor) vs normalized response-variable slope" module.

2.3. Sample generation and mRNA sequencing

All sample replicates used for mRNA sequencing were grown in a single culture batch. This included three replicates of the ALB-S (DMSO) control, and because higher ALB-R cultures showed reduced growth rate, eight replicates of the ALB-R isolate. All cultures were grown in

Falcon t25 flasks in 56 mL of fresh TYI medium and incubated at 37 °C for ~60 h. ALB-S cultures were seeded with 10^5 trophozoites and reached confluence at harvesting. ALB-R required an initial seeding of 1.5–3 × 10^6 trophozoites, which were grown in ALB at a final concentration of 0.5 μM and harvested at 60 h regardless of whether they achieved full confluence. After incubation, flasks were inverted, and supernatant and suspended trophozoites (likely to contain dead/dying and dividing cells, which could confound the mRNA integrity and comparative transcription analyses, respectively) were decanted to waste; 50 mL of ice-cold complete TYI medium were added, and flasks were incubated on ice-water for 10 min to detach trophozoites. The suspended cells were transferred to 50 mL falcon tubes and pelleted (680×*g*, 5 min, 4 °C). The supernatant was removed, and pellets were re-suspended, transferred to UV-irradiated 1.5 mL microfuge tubes, and pelleted (720×*g*, 2 min, RT). Samples from ALB-R lines were consolidated into three microfuge tubes to form the requisite replicates for sequencing. The supernatant was removed, and the pellets dissolved in 1 mL of TriPure reagent (Roche), incubated at RT for 5 min, and stored at −80 °C.

RNA was extracted according to the TriPure (Sigma-Aldrich) manufacturer's protocol within 4 weeks of sample preparation. The dried RNA pellet was re-suspended in reverse-osmosis deionized water (H_2O) and treated with Turbo DNAse (Ambion) according to the manufacturer's instructions. RNA concentration was estimated by fluorometry (Qubit), and quality control was performed using a BioAnalyzer (Agilent). Polyadenylated RNA was purified from 10 μg of total RNA using Sera-mag oligo (dT) beads, fragmented to a length of 100–500 bases, and reverse transcribed using random hexamers. Strands were labelled using the dUTP second-strand synthesis method, end-repaired and adaptor-ligated, and then treated with uracil-specific excision reagent (USER; NEB) before amplification by PCR. Products were purified over a MinElute column (Qiagen), and single-end sequencing was performed using an Illumina HiSeq 2500 (YourGene Biosciences, Taiwan).

2.4. Data processing and analysis

Raw reads for each replicate (mean of 31 million reads) were assessed for quality by FastQC (Andrews, 2010). Trimmomatic (Bolger et al., 2014) was used to trim the adapters and low-quality bases (sliding window: 4 nt; minimum average PHRED quality: 20; leading and trailing: 3 nt; minimum read length: 40 nt). Filtered reads were mapped as single-ended reads to the non-deprecated coding genes described for the *G. duodenalis* WB genome GiardiaDB release 47 (Morrison et al., 2007; Aurrecoechea et al., 2009) using Rsubread (Liao et al., 2019) with "subread-align" (minimum fragment length of 10; maximum 4 mismatched bases; hit report consensus threshold by 1; maximal 2 equally-best mapping locations). Sense strand mapped read counts were generated for each gene by "featureCounts" -s 2. The mapped reads were then submitted to edgeR (Robinson et al., 2010) for further analysis. Low-abundance transcripts were removed to reduce false discovery during differential transcriptional analysis, using the edgeR function' filterByExpr', which retained genes with counts per million (CPM) more than 0.37 across the smallest group sample size (equating to at least 10 counts per median library size) (Supplementary Fig. 1A). Libraries were normalized by Trimmed Mean of M-values (TMM) normalization (Supplementary Fig. 1B), followed by unsupervised clustering by limma (Ritchie et al., 2015) according to leading $\log_2$ fold change ($\log_2$-FC) dimensions (Supplementary Fig. 1C). Normalized counts were further adjusted by voom to remove identifiable technical variation (Supplementary Fig. 1D; Table S2). Differentially transcribed genes (DTGs) between the ALB-S and ALB-R conditions were identified using the emBayes test module at a false discovery rate (FDR) of 0.05 and a minimum absolute $\log_2$-FC of more than 1. SNP calling of TUB1 was performed by "exactSNP" in Rsubread by default threshold (base quality score at 13; q-value at 12).

Hypothetical proteins identified among the DTGs that were less than 750 amino acids were queried for functional annotations based on structural homology modelling for *G. duodenalis* (Ansell et al., 2019). Larger hypothetical proteins not included in this previous study (Ansell et al., 2019) were analyzed by Phyre2. DAVID (Huang et al., 2009) was used for domain and molecular function enrichment analysis for DTGs. Romer (Wu et al., 2010) was used to test the enrichment of Gene Ontology (GO) terms and KEGG pathways throughout the whole transcriptome (here termed as "functional trend analysis") in susceptible and resistant lines (significance threshold: adjusted P value less than 0.05, minimum cluster size more than 5 genes). The raw RNA-sequence reads relating to this study are available at https://www.ncbi.nlm.nih.gov/bioproject/PRJNA951805.

3. Results and discussion

Selection for ALB-R *G. duodenalis* WB-1B trophozoites required six incremental increases in continuous, sublethal ALB concentration from 0.1 to 0.5 μM over 315 days, followed by stabilization at 0.5 μM (Supplementary Fig. 2A). Following this stabilization period, we measured a 12-fold increase in the ALB IC50 for the ALB-R compared to the WB ALB-S (DMSO) control (Supplementary Fig. 2B). In a previous study (Emery-Corbin et al., 2021b), we identified a statistically significant increase in the frequency of a TUB1 SNP, E198K, in this ALB-R isolate relative to its ALB-S parental line. We also demonstrated that this SNP frequency was positively correlated with increasing resistance factor at 3 discrete points of stabilization during sublethal ALB selection. This SNP has been linked to ALB-R acquisition in some fungal species (Yarden and Katan, 1993; Banno et al., 2008; Cai et al., 2015). Extending this work here, we explored the transcriptomic differences between these isolates to better understand the ALB-R mechanism. To do this, we generated 30.7–31.3 M strand-specific RNA-seq reads per replicate (three ALB-S DMSO controls and three ALB-R), with 81.8–84.3% of these representing sense strand transcripts from the annotated coding domains of the *G. duodenalis* WB reference genome (GiardiaDB release 47) (Table S1). In total, 5599 genes were identified as transcribed at more than 0.37 counts per million (CPM) in all replicates following normalization (Table S2). Notably, the E198K SNP in TUB1 was detected at an allelic frequency ~45% in the transcripts of the ALB-R replicates and absent from all ALB-S replicates (Supplementary Fig. 3).

We used two major approaches to explore changes in the *G. duodenalis* WB-1B transcriptome associated with *in vitro* selected ALB-R. Firstly, using conventional gene-based analyses with pairwise statistical analysis, we identified 290 differentially transcribed genes (DTGs: FDR <0.05 and absolute $\log_2$-FC > 1) between ALB-S and ALB-R replicates, with 155 of these up- and 135 down-regulated in ALB-R (Fig. 1A; Tables S3–S4). Next, we explored functional trends among these statistically significant DTGs using conserved protein domain and Gene Ontology (GO) enrichment analysis (Fig. 1B–C, Table S7).

Secondly, we undertook a broader, functional trend analysis of the overall transcriptome (Fig. 2A–B; Tables S9–S51), independent of the statistical status of individual genes as determined in the first analysis. This approach grouped the transcripts into functional clusters based on their GO terms or KEGG pathway classification. We then tested which, if any, of these transcript clusters were statistically significantly more highly ('up'), lowly ('down') or bimodally ('mixed') transcribed relative to the overall transcriptome in ALB-R vs ALB-S replicates (Tables S10–S11). A detailed account of all transcriptional changes, along with the corresponding heatmaps of each functional cluster in the trend analysis, can be found in Tables S9–S51. Using our gene-focused and trend-focused analyses, we have then explored how these may provide mechanistic context for ALB MOA and the resistance mechanism.

3.1. Major VSPs turnover with ALB-R

Variant-specific surface proteins (VSPs) featured prominently among

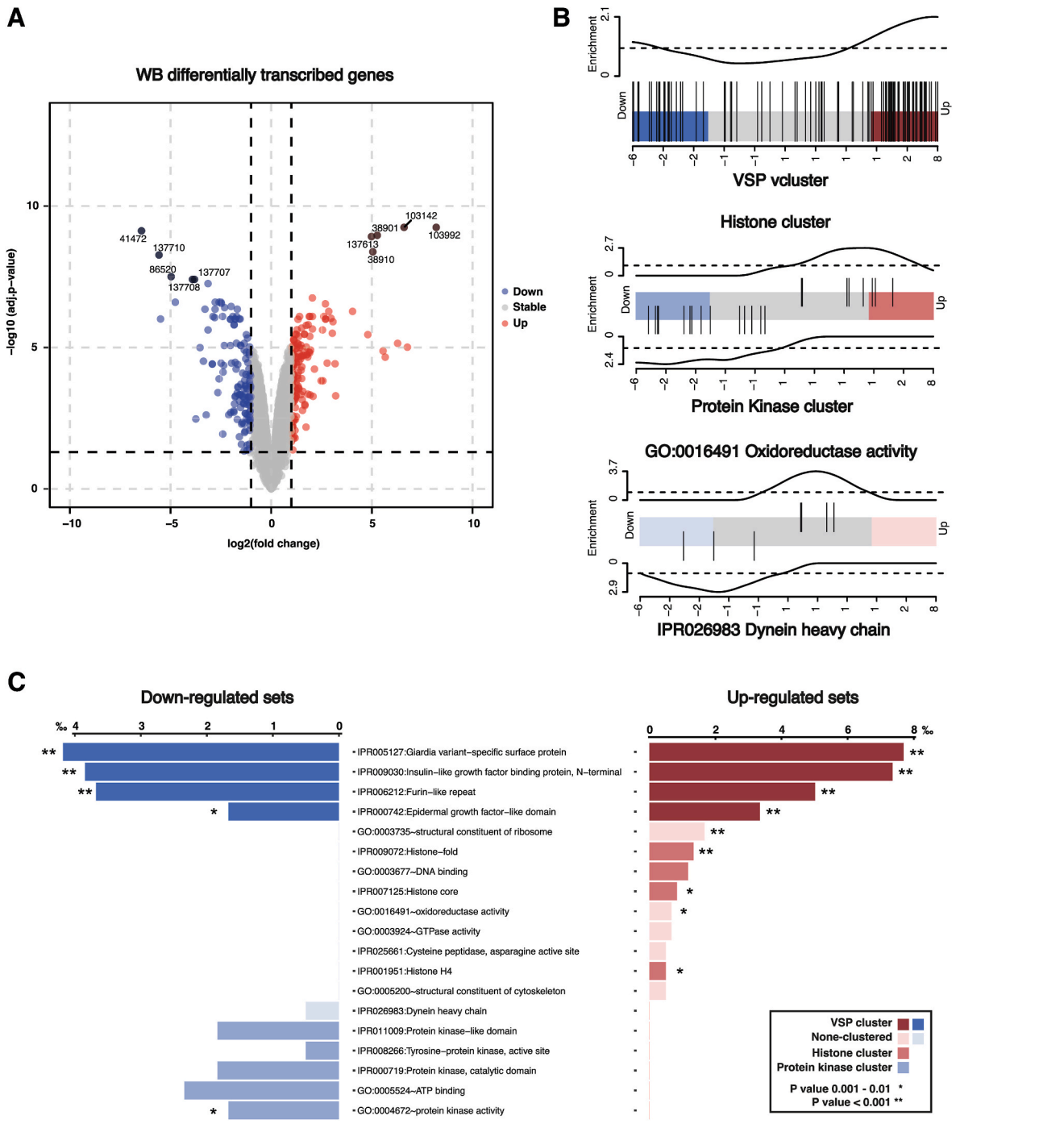

Fig. 1. Differentially expressed genes between ALB-S and ALB-R lines. (A) 155 up- and 135 down-regulated genes under FDR <0.05 and absolute $\log_2$-FC > 1. The top/bottom five genes are labelled. (B) Significantly enriched gene sets of molecular and domain function in DTGs under a P value less than 0.01. Gene numbers over the whole genome are shown in bars. Gene sets containing overlapped genes or related functions have been shaded into different clusters. (C) Log2 fold change distribution of varying gene sets clusters and representative gene sets.

up- and down-regulated transcripts. Nine of the ten most differentially transcribed genes (five up- and four down-regulated) are VSPs (Fig. 1A). Functional enrichment analyses identified VSPs and VSP-associated conserved protein domains (IPR009030, IPR6212 and IPR000742) as statistically significantly enriched among up- and down-regulated genes (Fig. 1B). Gene-set enrichment analysis also revealed a bimodal transcriptional pattern among *G. duodenalis* WB-1B's VSPs (Fig. 1C). These data appear consistent with a major switching (some genes up- and others down-regulated) of transcribed VSPs within ALB-R, as has been observed previously (Argüello-García et al., 2009). Such switching events have been described previously in *G. duodenalis* in various contexts, including MTZ-R, response to various external stress stimuli, and encystation (Ansell et al., 2016, 2017; Einarsson et al., 2016; Balan et al., 2021). These may have functional relevance to ALB-R specifically but more likely reflect some aspect of a common mechanism through which *G. duodenalis* mounts major transcriptomic changes. Many high cysteine membrane proteins (HCMPs) up-regulated during host-parasite interactions are also up-regulated here (GL_101589, GL_114470, GL_112135, GL_7715, GL_137727, GL_114930, GL_115066) (Peirasmaki et al., 2020). Notably, VSP expression is heavily regulated through

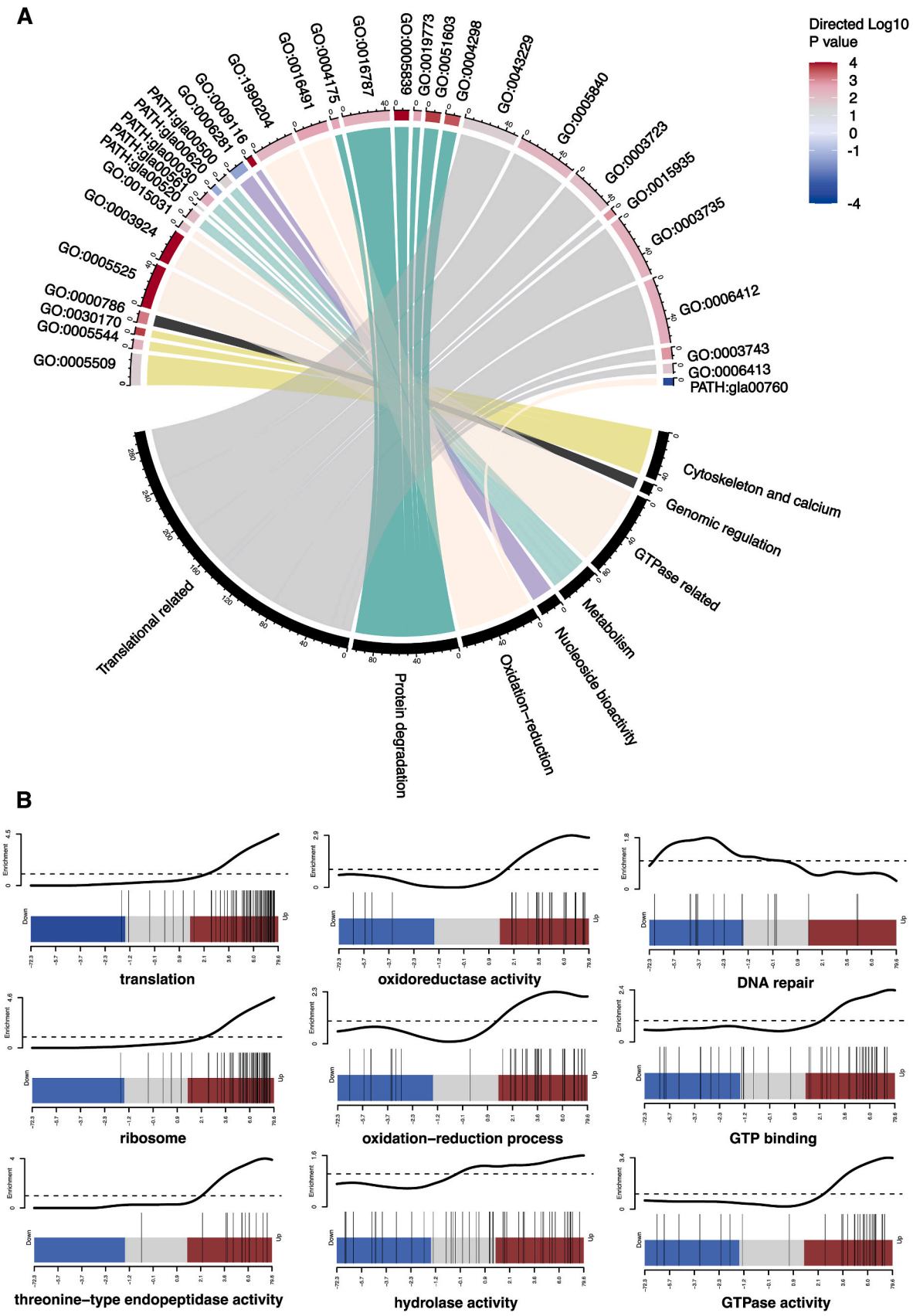

(caption on next page)

Fig. 2. Unbiased global gene sets enrichment analysis summarized in chord plot. (A) Twenty-five gene ontology terms and 6 KEGG metabolism pathways are significantly enriched in ALBR lines, according to Romer. Directed enrichment p-value of all 31 gene sets are plotted in the upper grid where the positive value represents up-regulated gene sets, and the negative value represents down-regulated gene sets. More absolute log10 p-value represents more significance. Terms have further been classified into translation (translational initiation GO:0006413, translation GO:0006412, ribosome GO:0005840, small ribosomal subunit GO:0015935, intracellular GO:0043229. Translation initiation factor activity GO:0003743. RNA binding GO:0003723, structural constituent of ribosome GO:0003735), protein degradation (proteolysis involved in cellular protein catabolic process GO:0051603, proteasome core complex, alpha-subunit complex GO:0019773, proteasome core complex GO:0005839, threonine-type endopeptidase activity GO:0004298, endopeptidase activity GO:0004175, hydrolase activity GO:0016787), genomic regulation (nucleosome GO:0000786), carbohydrate metabolism (Amino sugar and nucleotide sugar metabolism PATH:gla00520, Glycerolipid metabolism PATH:gla00010, Pentose phosphate pathway PATH:gla00030, Starch and sucrose metabolism PATH:gla00500, Pyruvate metabolism PATH:gla00620), oxidation-reduction (oxidation-reduction process GO:1990204, oxidoreductase activity GO:0016491, Nicotinate and nicotinamide metabolism PATH:gla00760), GTPase related (GTP binding GO:0005525, GTPase activity GO:0003924, protein transport GO:0015031), cytoskeleton and calcium (calcium ion binding GO:0005509, calcium-dependent phospholipid binding GO:0005544, pyridoxal phosphate binding GO:0030170), and nucleoside metabolism (nucleoside metabolic process GO:0009116, DNA repair GO:0006281). (B) Barcode plot of t-statistics for representative GO terms.

post-transcriptional RNA interference (Prucca et al., 2008). Possibly consistent with major changes in genetic regulation, we noted histone genes, including two copies of H2A and H2B, one H3 and three copies of H4, are up-regulated with ALB-R (Fig. 1; Table S3). We also see significant switching in *G. duodenalis* WB-1B's histone modifiers (Emery-Corbin et al., 2021a) and major transcription regulators (Einarsson et al., 2016) in our functional trend analyses (Table S14).

3.2. Changes in microtubule-associated transcription primarily focused on disc and basal bodies

ALB-exposure results in significant ultrastructural changes in the *G. duodenalis* trophozoite (Chavez et al., 1992; Oxberry et al., 1994). These changes include enlargement or rounding of the cell and aberrant localization of the basal bodies and flagella. However, the most pronounced of these changes is the fragmentation and disintegration of the adhesive disc. Consistent with TUB1 being the primary target of ALB in various eukaryotes (Chatterji et al., 2011), microtubule cytoskeleton-related genes are the second largest group among the DTGs in *G. duodenalis* WB-1B and include 20 up- and five down-regulated transcripts (Tables S3–S5). Eleven of the 25 cytoskeletal proteins differentially transcribed in *G. duodenalis* WB-1B with ALB-R have been localized in the trophozoite (Dawson and House, 2010; Hagen et al., 2020). Six of these are specific to the adhesive disc, including β, δ and γ-giardin, SALP-1, a protein 21.1 (GL_17551) and a hypothetical protein (GL_15499). The remainder included two α-tubulins distributed throughout the cell (Woessner and Dawson, 2012), and proteins localizing to the basal body (protein 21.1 GL_17053 and GL_24412) or axoneme (GL_24412 and dynein GL_17243). Microtubule-associated DTGs lacking a known cellular localization in *Giardia* included six protein 21.1s, three dynein heavy chains, two Mec-17 α-tubulin N-acetyltransferases (GL_117391, GL_117392), dynamin, radial spoke protein, a putative gamma-tubulin complex component 4 (GL_42368), and a calmodulin that binds α-tubulin during encystation and is up-regulated at the G2 phase of wild type *G. duodenalis* (Alvarado and Wasserman, 2012; Kim and Park, 2019). Notably, β-giardin, δ-giardin and SALP-1 comprise the SF-assembling complex (Holberton et al., 1988; Nosala et al., 2020), which in *G. duodenalis* is primarily involved in the formation of microtubule-based microribbons at the margins of the adhesive disc (Nosala et al., 2018). Fragmentation of the microribbons is one of the earliest structural artefacts associated with ALB exposure in this parasite (Oxberry et al., 1994). Indeed, mutations in β-giardin have been linked to ALB-R (Jiménez-Cardoso et al., 2009). This pattern was also reflected in the cytoskeletal microtubule heatmap overview (Table S20).

Consistent with the transcriptional changes among *G. duodenalis* WB-1B's tubulins, we observed a notable switching with ALB-R in the transcription of several NEK kinases, which phosphorylate tubulins and regulate microtubule stability (Westermann and Weber, 2003; Fry et al., 2012). Six *G. duodenalis* NEKs were up- (two active NEK and four dead NEK) and 11 down-regulated (five active NEK and six dead NEK) with ALB-R (Table S3-S4, S6). The observation of differential transcription among so-called 'dead' NEK kinases with ALB-R is intriguing. Dead NEKs lack critical catalytic residues in their putative, kinase-binding domain, suggesting they do not engage in phosphorylation (Manning et al., 2011). Their function in *G. duodenalis* is unknown, although it is notable that this family has radiated to a similar degree as the active NEKs in the *G. duodenalis* genome (Manning et al., 2011). Some pseudokinases, including protist NEKs (Westermann and Weber, 2002, 2003), are glutamyltransferases that glutamylate tubulins to regulate microtubule diversity and function (Kann et al., 2003; Black et al., 2019). However, although *G. duodenalis* glutamylates its tubulins (Boggild et al., 2002), the enzymes regulating this process have not been identified. Whether there is a role for pseudoNEK mediated post-translational modification of tubulins in *G. duodenalis* WB-1B's development of ALB-R is not known but is worthy of further exploration.

3.3. ALB-R correlates with markers of major protein turnover

We note the up-regulation of key pathways associated with protein degradation and turnover and elevated protein expression with ALB-R (Figs. 1 and 2). This includes statistically significant increases in (Tables S9 and S13) genes associated with the proteasome, protein catabolism, threonine endopeptidase activity and hydrolases. We also note the up-regulation of cathepsin B (GL_10217, GL_16779 and GL_14019), Xaa-Pro peptidase and dipeptidyl peptidase, which are major activities of secreted proteases that are involved in amino acid metabolism. In addition, we find significant enrichment of GO terms associated with the ribosome and statistically significant upward trends in functional terms related to the ribosome, translation, translational initiation and RNA-binding (Tables S3, S4, S9, S12), noting that the majority of ribosomal proteins have RNA-binding domains allowing their interaction with the rRNAs (Gerstberger et al., 2014). Although it is impossible to infer which specific proteins may be affected in our data, it seems likely that at least some of these changes are linked to the substantial changes in the transcription of major structural proteins associated with the *G. duodenalis* cytoskeletal system noted above.

3.4. Altered transcription of membrane and vesicle transport with ALB-R

Many GO terms trending upward in ALB-R included calcium ion binding, calcium-dependent phospholipid binding, and pyridoxal phosphate binding (Fig. 2; Tables S9 and S19). The genes associated with this function included several α-giardins and calcium binding-related genes (calmodulin, centrin, calcineurin and caltractin) (Friedberg, 2006). Indeed, all but one (α5-giardin) of *G. duodenalis'* 21 α-giardins trended upward in ALB-R (Table S19). Alpha-giardins are annexin-homologs and major components of the *G. duodenalis* cytoskeleton (Weiland et al., 2005; Kim and Park, 2019). Annexins bind phospholipids in the presence of calcium ions, interact with actin and are associated with membrane turnover, repair, and membrane/vesicular trafficking (Rescher and Gerke, 2004; Futter and White, 2007; Mirsaeidi et al., 2016; Koerdt et al., 2019). Calmodulin is a highly conserved primary sensor of calcium (Alvarado and Wasserman, 2012). In *G. duodenalis,* calmodulin GL_5333 localizes to the basal bodies and is

essential for motility, metabolism, and cytoskeleton activities (Lauwaet et al., 2011; Alvarado and Wasserman, 2012).

Consistent with this trend analysis, several vesicular and membrane-associated protein-coding genes are differentially transcribed between ALB-S and ALB-R. Eleven of these are up-regulated and include three cathepsin B precursors, two tenascin precursors, mucin-like protein, bet5-like protein, TM efflux protein, Xaa-Pro dipeptidase, permeability-increasing protein (GL_112630), and a putative cholesterol transport protein (GL_5800) (Ma'ayeh et al., 2017) (Table S3). Conversely, seven are down-regulated, including two ABC transporters, two cathepsin L precursors, permeability-increasing protein (GL_102575), sodium/bile acid symporter (GL_86933), and proprotein convertase subtilisin/kexin type 5 precursor (PCSK5, GL_114625) (Table S4). Further to this, cluster-based analyses identified GTPase activity (GO:0003924) as enriched among the DTGs up-regulated with ALB-R (Fig. 1C), and functional trend analysis found that *Giardia duodenalis* WB-1B's GTPases trended up with ALB-R (Table S18). Most of these upwardly trending GTPases are Rab GTPases, which regulate the direction and specificity of vesicle trafficking (Stenmark, 2009).

Altered transcription of genes involved in membrane trafficking and repair could be consistent with observations that oxidative ALB or its metabolites cause damage to macromolecules, including the lipid bilayers (Martinez-Espinosa et al., 2015) and may support the involvement of the oxidative stress response in ALB-R in *G. duodenalis* (Argüello-Garcia et al., 2015). However, they may also indicate disruption of vesicular trafficking, consistent with the suspected MOA of ALB in multicellular parasites, such as parasitic nematodes, in which it is thought to cause starvation through a disruption of the vesicular transport of glucose (Jasra et al., 1990). We explore changes in transcription associated with metabolism and oxidative stress responses in more detail below.

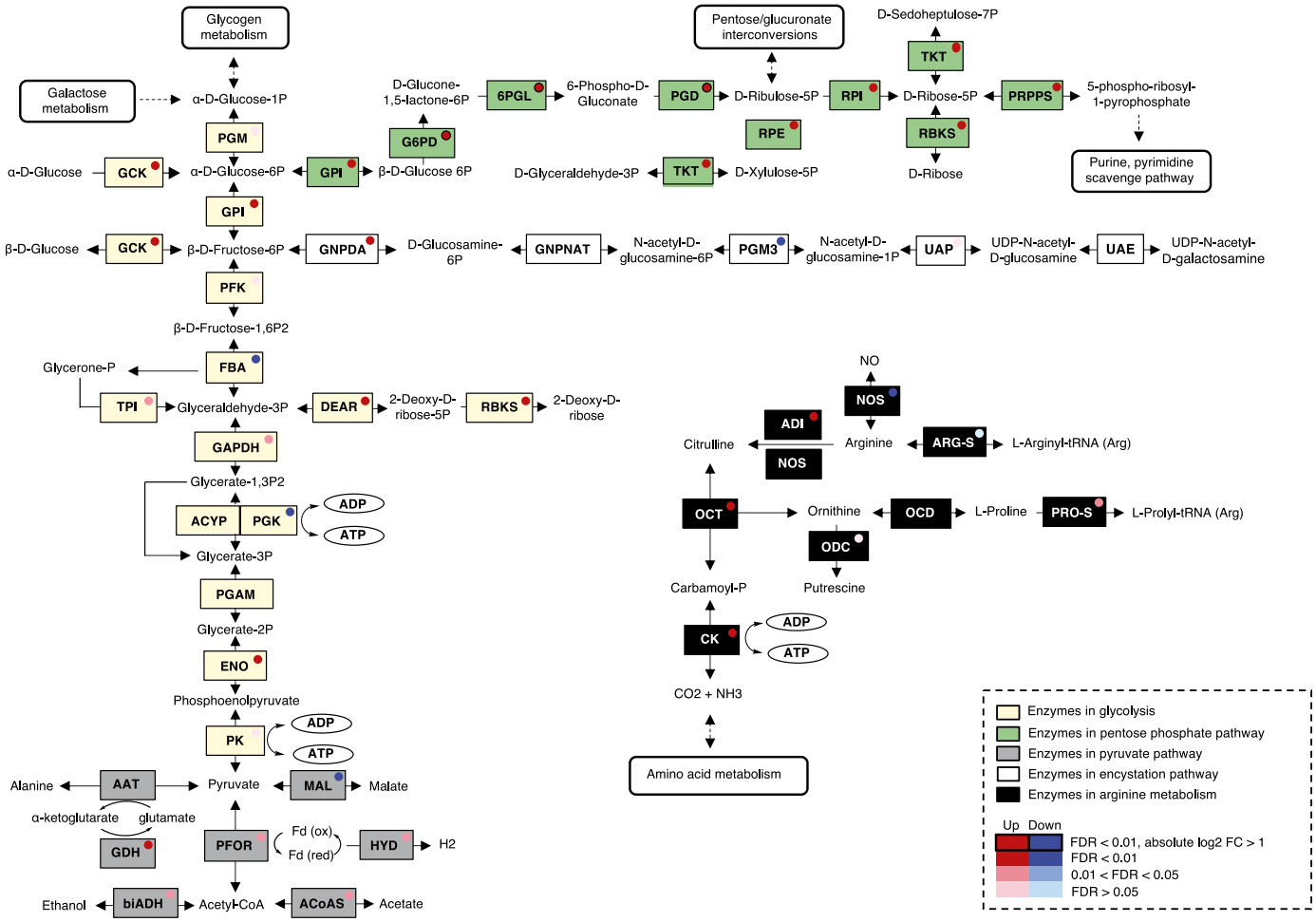

Fig. 3. Mapping transcript variations on glycolysis, PPP, pyruvate, and arginine metabolic pathway. 6PGL, 6-phosphogluconolactonase, NO homolog; ACYP, acylyphosphatase, GL_5359, GL_7871; ADI, arginine deiminase, GL_112103; ARG-S, arginyl-tRNA synthetase, GL_10521; CK, carbamate kinase, GL_16453; DERA, deoxyribose-phosphate aldolase, GL_15127; ENO, enolase, GL_11118; FBA, fructose-bisphosphate aldolase, GL_11043; G6PD, glucose-6-phosphate dehydrogenase, GL_8682; GAPDH, glyceraldehyde-3-phosphate dehydrogenase, GL_17043, GL_ 6687; GCK, glucokinase, GL_8826; GNPDA, glucosamine-6-phosphate deaminase, GL_10829, GL_8245; GNPNAT, glucosamine 6-phosphate N-acetyltransferase, GL_14651; GPI, glucose-6-phosphate isomerase, GL_9115; NOS, nitric oxide synthase, GL_91252; OCD, ornithine cyclodeaminase, GL_2452; OCT, ornithine carbamoyltransferase, GL_10311; ODC, ornithine decarboxylase, GL_94582; PFK, phosphofructokinase (pyrophosphate-based), GL_14993; PGAM, phosphoglycerate mutase, GL_8822; PGD, phosphogluconate dehydrogenase, GL_14759; PGK, phosphoglycerate kinase, GL_90872; PGM, phosphoglucomutase, GL_16069, GL_17254; PGM3, phosphoacetylglucosamine mutase, GL_16069; PK, pyruvatekinase, GL_3206, GL_17143; PRO-S, prolyl-tRNAsynthetase, GL_15983; PRPPS, phosphoribosylpyrophosphate synthetase, GL_21750; RBKS, ribokinase, GL_15297; RPE, ribulose-phosphate 3 epimerase, GL_ 10324; RPI, ribose-5-phosphate isomerase, GL_27614; TKT, transketolase, GL_9704; TPI, triose phosphate isomerase, GL_93938; UAE, UDP-N-acetylglucosamine 4-epimerase, 5.1.3.7; UAP, UDP-N-acetylglucosamine diphosphorylase, GL_16217; PFOR, pyruvate:ferredoxin oxidoreductase (Pyruvate-flavodoxin oxidoreductase), GL_17063, GL_114609; GDH, NADP-specific glutamate dehydrogenase, GL_21942; MAL, malic enzyme, GL_14285; HYD, hydrogenase, GL_6304; ACoAS, acetyl-CoA synthetase, GL_16667, GL_13608; AAT, alanine aminotransferase, GL_12150, GL_16353.

3.5. A potential shift from glycolysis to arginine metabolism for ATP production with ALB-R

Giardia duodenalis is an obligate microaerophile (Morrison et al., 2007; Ankarklev et al., 2010) that lacks conventional mitochondria (Tovar et al., 2003). The primary mode of ATP generation is through fermentative glycolysis driven by a small suite of enzymes, such as PFOR, that contain an iron-sulphur (Fe–S) core (Ansell et al., 2015b). Ironically, the metabolic adaptations that allow *G. duodenalis* to exploit a low-oxygen environment also make it highly susceptible to oxidative stress. Fe–S clusters, in particular, are susceptible to oxidation. Many core players in *G. duodenalis'* central carbon metabolism also play key roles in its stress responses (Ansell et al., 2016). This is intriguing biology but is also highly relevant when considering that the ALB MOA may include starvation through the inhibition of the vesicular glucose transport (Jasra et al., 1990) or the induction of oxidative stress (Martinez-Espinosa et al., 2015).

To better understand if these changes reflected altered metabolic activity, stress responses or both, we first undertook a more detailed characterization of broader trends within *G. duodenalis* WB-1B's core carbon metabolism. Functional trend analysis identified significant upward trends with ALB-R in the transcription of essential genes driving glucose and arginine metabolism (Fig. 3; Tables S3, S4, S15, S17). Next, we mapped these overall trends to the *G. duodenalis* glucose metabolism pathways (Fig. 3) to better understand their implications. Notably, all genes within the pentose phosphate pathway (PPP) trended upward with ALB R. Each of these was statistically significant (FDR <0.01) and up-regulated in our DTG analysis. However, only glucose-6-phosphate 1-dehydrogenase (G6PD, GL_8682 or 6-phosphogluconolactonase, 6GPL as per (Xu et al., 2020)) and 6-phosphogluconate dehydrogenase decarboxylating (PGD, GL_ 14759) reached the minimum absolute fold-change cut-off ($\log_2$FC > 1). In contrast, the trend behaviour of genes involved in core glycolysis is mixed and includes the notable but subtle down-regulation (FDR <0.05 but $\log_2$FC < 1) of phosphoglycerate kinase (PGK), as one of the key producers of ATP in core glycolysis. Notably, ALB-R is marked by a significant up-regulation of arginine deiminase (ADI, GL_112103) and subtle but statistically significant up-regulation (FDR <0.01 but $\log_2$FC < 1) of ornithine-carbamyl transferase (OCT, GL_10311) and carbamate kinase (CK, GL_16453). In *G. duodenalis*, these enzymes provide a critical, alternative source of ATP production (Morrison et al., 2007) (Fig. 3). This result is consistent with previous work identify the down-regulation of triosephosphate isomerase in *Giardia duodenalis* with ALB-R coinciding with the up-regulation of ornithine carbamoyl transferase and phosphoglycerate kinase (Paz--Maldonado et al., 2013).

These changes are consistent with a shift in the primary source of ATP production with ALB-R in *G. duodenalis* WB-1B. However, the cause of this shift is not immediately apparent and requires further consideration. On the one hand, among helminths, ALB primarily functions by disrupting microtubules associated with glucose transport vesicles (Borgers and De Nollin, 1975). As noted above, we observe changes in transcriptional trends associated with the vesicular trafficking systems within the ALB-R *G. duodenalis* WB-1B line, which may be consistent with these observations in helminths. However, it is unclear how much a single-celled organism, such as *G. duodenalis,* might rely on vesicle trafficking for glucose uptake. Therefore, we thought to look at the behaviour of glucose and other sugar transporters in our dataset. However, these transporters are not well annotated in *G. duodenalis*. To overcome this, we used homolog-based matching against a panel of prokaryotic and eukaryotic sugar transporters (Landfear, 2010; Holman, 2020; Jeckelmann and Erni, 2020) to better annotate these genes in *G. duodenalis*. We identified two glucose transporter (GLUT) orthologs in *G. duodenalis* WB-1B (GL_5164 and GL_11540) alongside 22 additional genes with putative orthology to sugar transporters of various bacteria (Table S8). None of these was identified as statistically significantly up-regulated with ALB-R. However, GL_21411 and GL_112692 were among the down-regulated DTGs. Both are putative homologs of bacterial galactose/methyl-galactose import ATP-binding proteins (Table S4). Overall functional trend analysis indicated a potential switching in the transcriptional behaviour of *G. duodenalis* WB-1B's putative sugar transport repertoire. However, the trend was mixed, and it is unclear how to interpret these results (Table S17).

3.6. Does ALB-R involve the oxidative stress response in G. duodenalis?

Aside from glucose starvation, an alternative explanation for the down-regulation of core glycolytic enzymes and increased reliance on arginine metabolism for ATP in *G. duodenalis* WB-1B with ALB-R could be a response to oxidative stress. Oxidative stress due to BZs has been implicated previously as a part of ALB's MOA against *G. duodenalis* (Argüello-Garcia et al., 2015). Therefore, we looked at several aspects of the changes in the *G. duodenalis* WB-1B transcriptome with ALB-R to further investigate this possibility.

First, we looked at changes in the transcription of *G. duodenalis* WB-1B's oxidoreductases and other enzymes involved in its oxidative stress response. Our gene-based analyses identified enriched oxidoreductase activity (GO:0016491) among ALB-R up-regulated DTGs (Fig. 1). These up-regulated oxidoreductases were nitroreductase 1 (GL_22677) and 2 (GL_6175), an a-type flavoprotein lateral transfer candidate (GL_10358), a putative FMN binding protein (GL_5810), and a glutamate synthase (GL_7195). NR1 and 2 play critical roles in *G. duodenalis'* oxidative stress response (Ansell et al., 2015b) and are essential in metronidazole metabolism (Muller et al., 2013) and resistance (Ansell et al., 2015b). However, their transcriptional behaviour with ALB-R differs from that seen in metronidazole resistance (MtzR), in which NR2 is up- and NR1 down-regulated (Ansell et al., 2015a, 2017, 2019; Ibrahim et al., 2016). Overall trend-based analyses showed a bimodal transcriptional behaviour with ALB-R among *G. duodenalis* WB-1B's oxidoreductases (Table S16). ALB-R included the elevated transcription of thioredoxin, FMN-dependent, Fe–S-dependent and H_2O_2 detox-type enzymes. These appear to centre around the detoxification of H_2O_2 to NH_3 via NO, which has been implicated in BZ MOA in *Giardia duodenalis* in prior studies (Argüello-García et al., 2020). Notably, these transcriptional changes were subtle, and although many of the genes involved in H_2O_2-degradation met the cut-off for statistical significance (FDR <0.05) they did not meet the absolute fold-change cut-off ($\log_2$FC > 1). Interestingly, the enzymes required for H_2O_2 degradation requires NADH as a source of reducing power, which must be generated from the oxidized pool of NAD (Ansell et al., 2015b; Xie et al., 2020). However, we observed a downward trend in the transcription of enzymes that regulate salvage and conversion of NAD to NADH (Supplementary Fig. 4A, Table S17).

To further assess whether *G. duodenalis* WB-1B ALB-R responses are consistent with an oxidative stress response, we looked more closely at the behaviour of its Fe–S cluster enzymes. Under oxidative stress, these enzymes must be protected and are highly down-regulated at the transcript (Ansell et al., 2016, 2017) and protein level (Emery et al., 2018). *Giardia duodenalis* encodes four genes with a two iron two sulphur (Fe_2S_2) and 11 genes with a four iron four sulphur (Fe_4S_4) cluster (Supplementary Fig. 4B). Contrary to expectation, trend analysis identified a statistically significant overall elevation in the transcription of Fe–S cluster enzymes with ALB-R in *G duodenalis* WB-1B (Supplementary Figs. 4C–4D). Notably, we also identified the down-regulation of N-glycosylase/DNA lyase (GL_14544) and FEN-1 nuclease (GL_5488) with ALB-R. N-glycosylase/DNA lyase is a DNA repair enzyme that removes 8-oxoguanine, which accumulates on DNA damaged through oxidative stress (Machado-Silva et al., 2016) and is reported in *G. duodenalis* in a dose-dependent correlation with ALB exposure (Martinez-Espinosa et al., 2015). FEN-1 removes 5′ overhangs from single-stranded DNA during base excision repair (Liu et al., 2005) and should be up-regulated under H_2O_2 stress (Ansell et al., 2017). Collectively, these observations do not appear consistent with a cell under active oxidative or H_2O_2 stress. However, further transcriptomic studies

of ALB-R *G. duodenalis* isolates with and without the E198K or other TUB1 mutations is needed to determine whether the differences we observe for *G. duodenalis* WB-1B compared to prior ALB-R literature for this species reflect the isolate, the presence of E198K or another cause.

4. Concluding summary

Our study explored global transcriptomic changes in *Giardia duodenalis* WB-1B lineage with the *in vitro* acquisition of ALB resistance relative to its isogenic parental line. We found evidence of a transcriptional response incorporating many changes consistent with the broad understanding of BZ MOA in eukaryotic cells and historical observation of the impact of these compounds on *Giardia* at the structural level. We note major changes in the transcriptional behaviour of many giardins and tubulins, specifically among proteins associated with basal bodies, the adhesive disc and microribbons, in *G. duodenalis* WB-1B. Targeted proteomic studies have shown that these cytoskeletal elements are the most heavily impacted by BZ treatment (Chavez et al., 1992; Oxberry et al., 1994; Chatterji et al., 2011). In addition, we noted changes in *G. duodenalis* WB-1B's metabolic behaviour with ALB-R, specifically including a possible shift away from glucose and toward arginine metabolism as the primary source of ATP, which is consistent with prior observations (Paz-Maldonado et al., 2013). This coincided with major changes in the transcription of genes associated with membrane and vesicular trafficking, which may be consistent with the impact that BZs have on vesicular uptake and transport of glucose in nematodes (Lacey, 1988). However, these mechanisms are not sufficiently well characterized in *Giardia* to conclude this here.

We explored the possibility of ALB or its oxidative metabolites contributing to the MOA of BZs in *G. duodenalis* WB-1B, and the potential role of an oxidative stress response in the acquisition of ALB-R, as has been proposed previously (Paz-Maldonado et al., 2013; Argüello-Garcia et al., 2015; Martinez-Espinosa et al., 2015). However, although we see some indication of the H_2O_2 neutralization pathway being up-regulated with ALB-R, in our opinion, the global changes do not appear consistent with an oxidative stress response. Our observations are consistent with drug activity assays we reported previously for the *G. duodenalis* WB ALB-S and ALB-R lines (Emery-Corbin et al., 2021b), with overlapping resistances across all BZ 5-position structural variants, including those which undergo metabolic conversions (Albendazole, Mebendazole) as well as for those which do not (Parbendazole, Oxibendazole). This does not discredit the metabolic Alb-R phenotype observed in other studies (Paz-Maldonado et al., 2013; Argüello-Garcia et al., 2015; Martinez-Espinosa et al., 2015; Pech-Santiago et al., 2022), but may indicate multiple independent mechanisms of ALB-R in *Giardia* that merit further study.

It is important to note that the ALB-R *G. duodenalis* WB-1B isolate characterized in our study has acquired an E198K mutation in the TUB1 allele (Emery-Corbin et al., 2021b). This mutation is demonstrated to confer carbendazim resistance in fungi, and we have previously hypothesised it likely alters BZ binding to microtubules in *Giardia*. Whether this may impact the global changes we see with ALB-R in this lineage is unclear, but it is notable that even in the presence of this mutation there are clearly wider transcriptional changes to other cellular processes. This is not unexpected given the allele frequency of the E198K mutation indicated it was not yet dominant in our 0.5 μM ALB line (<50% allele frequency), suggesting these additional molecular mechanisms are also supporting the ALB-R phenotype. Future studies focused on additional *G. duodenalis* isolates, with and without the E198K mutation, are needed, as are functional studies artificially introducing the E198K SNP into ALB susceptible *G duodenalis* culture lines. Furthermore, additional studies of current Alb-R lineages using 'omics based approaches and compatible functional experiments will help to better understand the extent to which these isolates have exploited alternative mechanisms to overcome BZ exposure and help to identify markers of BZ resistance that may be used in clinical diagnostics.

Author contributions

QS, LB and AJ conceived the work. LB generated experimental samples. QS and AJ did data analysis and interpretation. SE, BA, and ST assist with data analysis. SE, BB and SGS assist with data interpretation. QS and AJ drafted the article. All authors critically revised the article.

Declaration of competing interest

The authors declare the following financial interests/personal relationships which may be considered as potential competing interests: All authors listed have contributed to the research, have no conflict of interest or competing interests to declare, and have approved the manuscript for submission to IJPDDR. The funders of this study have had no role in its design, data collection and interpretation, and are listed in the manuscript's acknowledgements.

Acknowledgments

Q. Su's PhD scholarship was funded by the Melbourne Research Scholarship, University of Melbourne, Australia. AR Jex was funded by the Australian National Health and Medical Research Foundation Leadership Fellowship program (APP1194330), Victorian State Government Operational Infrastructure Support, Australia and the Australian Government National Health and Medical Research Council Independent Research Institute Infrastructure Support Scheme. SJ Emery-Corbin was funded by a Jack Brockhoff Foundation (Australia) Early Career Grant (ID JBF 4184, 2016). We gratefully acknowledge the Walter and Eliza Hall Research Institute, Australia, for topping up the scholarship and providing Edith Moffatt with student travel scholarships.

Appendix A. Supplementary data

Supplementary data to this article can be found online at https://doi.org/10.1016/j.ijpddr.2023.03.004.

References

Aguayo-Ortiz, R., Méndez-Lucio, O., Romo-Mancillas, A., Castillo, R., Yépez-Mulia, L., Medina-Franco, J.L., Hernández-Campos, A., 2013. Molecular basis for benzimidazole resistance from a novel β-tubulin binding site model. J. Mol. Graph. Model. 45, 26–37.

Allen Paris, M., Gottlieb, D., 1970. Mechanism of action of the fungicide thiabendazole, 2-(4′-thiazolyl) benzimidazole. Appl. Microbiol. 20, 919–926.

Alvarado, M.E., Wasserman, M., 2012. Calmodulin expression during Giardia intestinalis differentiation and identification of calmodulin-binding proteins during the trophozoite stage. Parasitol. Res. 110, 1371–1380.

Andrews, S., 2010. FastQC: A Quality Control Tool for High Throughput Sequence Data ([Online]).

Ankarklev, J., Jerlstrom-Hultqvist, J., Ringqvist, E., Troell, K., Svard, S.G., 2010. Behind the smile: cell biology and disease mechanisms of Giardia species. Nat. Rev. Microbiol. 8, 413–422.

Ansell, B.R., Baker, L., Emery, S.J., McConville, M.J., Svard, S.G., Gasser, R.B., Jex, A.R., 2017. Transcriptomics indicates active and passive metronidazole resistance mechanisms in three seminal Giardia lines. Front. Microbiol. 8, 398.

Ansell, B.R., McConville, M.J., Baker, L., Korhonen, P.K., Emery, S.J., Svard, S.G., Gasser, R.B., Jex, A.R., 2016. Divergent transcriptional responses to physiological and xenobiotic stress in Giardia duodenalis. Antimicrob. Agents Chemother. 60, 6034–6045.

Ansell, B.R., McConville, M.J., Baker, L., Korhonen, P.K., Young, N.D., Hall, R.S., Rojas, C.A., Svard, S.G., Gasser, R.B., Jex, A.R., 2015a. Time-dependent transcriptional changes in axenic Giardia duodenalis trophozoites. PLoS Neglected Trop. Dis. 9, e0004261.

Ansell, B.R., McConville, M.J., Ma'ayeh, S.Y., Dagley, M.J., Gasser, R.B., Svard, S.G., Jex, A.R., 2015b. Drug resistance in Giardia duodenalis. Biotechnol. Adv. 33, 888–901.

Ansell, B.R.E., Pope, B.J., Georgeson, P., Emery-Corbin, S.J., Jex, A.R., 2019. Annotation of the Giardia proteome through structure-based homology and machine learning. GigaScience 8.

Argüello-Garcia, R., Cruz-Soto, M., Gonzalez-Trejo, R., Paz-Maldonado, L.M., Bazan-Tejeda, M.L., Mendoza-Hernandez, G., Ortega-Pierres, G., 2015. An antioxidant response is involved in resistance of Giardia duodenalis to albendazole. Front. Microbiol. 6, 286.

Argüello-García, R., Cruz-Soto, M., Romero-Montoya, L., Ortega-Pierres, G., 2004. Variability and variation in drug susceptibility among Giardia duodenalis isolates and clones exposed to 5-nitroimidazoles and benzimidazoles in vitro. J. Antimicrob. Chemother. 54, 711–721.
Argüello-García, R., Cruz-Soto, M., Romero-Montoya, L., Ortega-Pierres, G., 2009. In vitro resistance to 5-nitroimidazoles and benzimidazoles in Giardia duodenalis: variability and variation in gene expression. Infect. Genet. Evol. 9, 1057–1064.
Argüello-García, R., Leitsch, D., Skinner-Adams, T., Ortega-Pierres, M.G., 2020. Chapter six - drug resistance in Giardia: mechanisms and alternative treatments for giardiasis. In: Ortega-Pierres, M.G. (Ed.), Adv Parasitol. Academic Press, pp. 201–282.
Aurrecoechea, C., Brestelli, J., Brunk, B.P., Carlton, J.M., Dommer, J., Fischer, S., Gajria, B., Gao, X., Gingle, A., Grant, G., Harb, O.S., Heiges, M., Innamorato, F., Iodice, J., Kissinger, J.C., Kraemer, E., Li, W., Miller, J.A., Morrison, H.G., Nayak, V., Pennington, C., Pinney, D.F., Roos, D.S., Ross, C., Stoeckert Jr., C.J., Sullivan, S., Treatman, C., Wang, H., 2009. GiardiaDB and TrichDB: integrated genomic resources for the eukaryotic protist pathogens Giardia lamblia and Trichomonas vaginalis. Nucleic Acids Res. 37, D526–D530.
Balan, B., Emery-Corbin, S.J., Sandow, J.J., Ansell, B.R.E., Tichkule, S., Webb, A.I., Svärd, S.G., Jex, A.R., 2021. Multimodal regulation of encystation in Giardia duodenalis revealed by deep proteomics. Int. J. Parasitol. 51, 809–824.
Banno, S., Fukumori, F., Ichiishi, A., Okada, K., Uekusa, H., Kimura, M., Fujimura, M., 2008. Genotyping of benzimidazole-resistant and dicarboximide-resistant mutations in botrytis cinerea using real-time polymerase chain reaction assays. Phytopathology® 98, 397–404.
Beech, R.N., Skuce, P., Bartley, D.J., Martin, R.J., Prichard, R.K., Gilleard, J.S., 2011. Anthelmintic resistance: markers for resistance, or susceptibility? Parasitology 138, 160–174.
Black, M.H., Osinski, A., Gradowski, M., Servage, K.A., Pawłowski, K., Tomchick, D.R., Tagliabracci, V.S., 2019. Bacterial pseudokinase catalyzes protein polyglutamylation to inhibit the SidE-family ubiquitin ligases. Science 364, 787.
Boggild, A., Sundermann, C., Estridge, B., 2002. Post-translational glutamylation and tyrosination in tubulin of tritrichomonads and the diplomonad Giardia intestinalis. Parasitol. Res. 88, 58–62.
Bolger, A.M., Lohse, M., Usadel, B., 2014. Trimmomatic: a flexible trimmer for Illumina sequence data. Bioinformatics 30, 2114–2120.
Borgers, M., De Nollin, S., 1975. Ultrastructural changes in Ascaris suum intestine after mebendazole treatment in vivo. J. Parasitol. 110–122.
Borgers, M., De Nollin, S., Verheyen, A., De Brabander, M., Thienpont, D., 1975. Effects of new anthelmintics on the microtubular system of parasites. Microtubules Microtubule Inhibitors 497–508.
Cai, M., Lin, D., Chen, L., Bi, Y., Xiao, L., Liu, X.-l., 2015. M233I mutation in the β-tubulin of botrytis cinerea confers resistance to zoxamide. Sci. Rep. 5, 16881.
Campanati, L., Troester, H., Monteiro-Leal, L.H., Spring, H., Trendelenburg, M.F., de Souza, W., 2003. Tubulin diversity in trophozoites of Giardia lamblia. Histochem. Cell Biol. 119, 323–331.
Capon, A.G., Upcroft, J.A., Boreham, P.F.L., Cottis, L.E., Bundesen, P.G., 1989. Similarities of Giardia antigens derived from human and animal sources. Int. J. Parasitol. 19, 91–98.
Chatterji, B.P., Jindal, B., Srivastava, S., Panda, D., 2011. Microtubules as antifungal and antiparasitic drug targets. Expert Opin. Ther. Pat. 21, 167–186.
Chavez, B., Cedillo-Rivera, R., Martinez-Palomo, A., 1992. Giardia lamblia: ultrastructural study of the in vitro effect of benzimidazoles. J. Protozool. 39, 510–515.
Davids, B.J., Gillin, F.D., 2011. Methods for Giardia culture, cryopreservation, encystation, and excystation in vitro. In: Luján, H.D., Svärd, S. (Eds.), Giardia: A Model Organism. Springer Vienna, Vienna, pp. 381–394.
Dawson, S.C., House, S.A., 2010. Chapter 17 - imaging and analysis of the microtubule cytoskeleton in Giardia. In: Cassimeris, L., Tran, P. (Eds.), Methods in Cell Biology. Academic Press, pp. 307–339.
Einarsson, E., Troell, K., Hoeppner, M.P., Grabherr, M., Ribacke, U., Svard, S.G., 2016. Coordinated changes in gene expression throughout encystation of Giardia intestinalis. PLoS Neglected Trop. Dis. 10, e0004571.
Elard, L., Humbert, J.F., 1999. Importance of the mutation of amino acid 200 of the isotype 1 β-tubulin gene in the benzimidazole resistance of the small-ruminant parasite Teladorsagia circumcincta. Parasitol. Res. 85, 452–456.
Emery, S.J., Baker, L., Ansell, B.R.E., Mirzaei, M., Haynes, P.A., McConville, M.J., Svard, S.G., Jex, A.R., 2018. Differential protein expression and post-translational modifications in metronidazole-resistant Giardia duodenalis. GigaScience 7.
Emery-Corbin, S.J., Hamey, J.J., Balan, B., Rojas-López, L., Svärd, S.G., Jex, A.R., 2021a. Eukaryote-conserved histone post-translational modification landscape in Giardia duodenalis revealed by mass spectrometry. Int. J. Parasitol. 51, 225–239.
Emery-Corbin, S.J., Su, Q., Tichkule, S., Baker, L., Lacey, E., Jex, A.R., 2021b. In vitro selection of Giardia duodenalis for Albendazole resistance identifies a β-tubulin mutation at amino acid E198K. Int. J. Parasitol.: Drugs Drug Resist. 16, 162–173.
Escobedo, A.A., Cimerman, S., 2007. Giardiasis: a pharmacotherapy review. Expet Opin. Pharmacother. 8, 1885–1902.
Friedberg, F., 2006. Centrin isoforms in mammals. Relation to calmodulin. Mol. Biol. Rep. 33, 243–252.
Fry, A.M., O'Regan, L., Sabir, S.R., Bayliss, R., 2012. Cell cycle regulation by the NEK family of protein kinases. J. Cell Sci. 125, 4423–4433.
Furness, B.W., Beach, M.J., Roberts, J.M., 2000. Giardiasis surveillance–United States, 1992–1997. MMWR CDC Surveill Summ 49, 1–13.
Furtado, L.F.V., de Paiva Bello, A.C.P., Rabelo É, M.L., 2016. Benzimidazole resistance in helminths: from problem to diagnosis. Acta Trop. 162, 95–102.
Futter, C.E., White, I.J., 2007. Annexins and endocytosis. Traffic 8, 951–958.
Gerstberger, S., Hafner, M., Tuschl, T., 2014. A census of human RNA-binding proteins. Nat. Rev. Genet. 15, 829–845.
Ghisi, M., Kaminsky, R., Mäser, P., 2007. Phenotyping and genotyping of Haemonchus contortus isolates reveals a new putative candidate mutation for benzimidazole resistance in nematodes. Vet. Parasitol. 144, 313–320.
Guerrant, R.L., DeBoer, M.D., Moore, S.R., Scharf, R.J., Lima, A.A., 2013. The impoverished gut—a triple burden of diarrhoea, stunting and chronic disease. Nat. Rev. Gastroenterol. Hepatol. 10, 220.
Hagen, K.D., McInally, S.G., Hilton, N.D., Dawson, S.C., 2020. Chapter two - microtubule organelles in Giardia. In: Ortega-Pierres, M.G. (Ed.), Adv Parasitol. Academic Press, pp. 25–96.
Holberton, D., Baker, D.A., Marshall, J., 1988. Segmented α-helical coiled-coil structure of the protein giardin from the Giardia cytoskeleton. J. Mol. Biol. 204, 789–795.
Holman, G.D., 2020. Structure, function and regulation of mammalian glucose transporters of the SLC2 family. Pflueg. Arch. Eur. J. Physiol. 472, 1155–1175.
Huang, D., Sherman, B.T., Lempicki, R.A., 2009. Systematic and integrative analysis of large gene lists using DAVID bioinformatics resources. Nat. Protoc. 4, 44–57.
Ibrahim, I.M., Puthiyaveetil, S., Allen, J.F., 2016. A two-component regulatory system in transcriptional control of photosystem stoichiometry: redox-dependent and sodium ion-dependent phosphoryl transfer from cyanobacterial histidine kinase Hik2 to response regulators Rre1 and RppA. Front. Plant Sci. 7.
James, C.E., Hudson, A.L., Davey, M.W., 2009. Drug resistance mechanisms in helminths: is it survival of the fittest? Trends Parasitol. 25, 328–335.
Jasra, N., Sanyal, S.N., Khera, S., 1990. Effect of thiabendazole and fenbendazole on glucose uptake and carbohydrate metabolism in trichuris globulosa. Vet. Parasitol. 35, 201–209.
Jeckelmann, J.-M., Erni, B., 2020. Transporters of glucose and other carbohydrates in bacteria. Pflueg. Arch. Eur. J. Physiol. 472, 1129–1153.
Jiménez-Cardoso, E., Eligio-García, L., Cortés-Campos, A., Flores-Luna, A., Valencia-Mayoral, P., Lozada-Chávez, I., 2009. Changes in beta-giardin sequence of Giardia intestinalis sensitive and resistant to albendazole strains. Parasitol. Res. 105, 25–33.
Kann, M.L., Soues, S., Levilliers, N., Fouquet, J.P., 2003. Glutamylated tubulin: diversity of expression and distribution of isoforms. Cell Motil Cytoskeleton 55, 14–25.
Keeling, P.J., Doolittle, W.F., 1996. Alpha-tubulin from early-diverging eukaryotic lineages and the evolution of the tubulin family. Mol. Biol. Evol. 13, 1297–1305.
Keister, D.B., 1983. Axenic culture of Giardia lamblia in TYI-S-33 medium supplemented with bile. Trans. Roy. Soc. Trop. Med. Hyg. 77, 487–488.
Khan, M., Ahmad, R., Rehman, G., Gul, N., Shah, S., Salar, U., Perveen, S., Khan, M.K., 2019. Synthesis of pyridinyl-benzo[d]imidazole/pyridinyl-benzo[d]thiazole derivatives and their yeast glucose uptake activity in vitro. Lett. Drug Des. Discov. 16, 984–993.
Kim, J., Park, S.-J., 2019. Role of gamma-giardin in ventral disc formation of Giardia lamblia. Parasites Vectors 12, 227.
Kim, U., Shin, C., Kim, C.Y., Ryu, B., Kim, J., Bang, J., Park, J.-H., 2021. Albendazole exerts antiproliferative effects on prostate cancer cells by inducing reactive oxygen species generation. Oncol. Lett. 21, 395.
Koerdt, S.N., Ashraf, A.P.K., Gerke, V., 2019. Chapter Three - annexins and plasma membrane repair. In: Andrade, L.O. (Ed.), Current Topics in Membranes. Academic Press, pp. 43–65.
Lacey, E., 1988. The role of the cytoskeletal protein, tubulin, in the mode of action and mechanism of drug resistance to benzimidazoles. Int. J. Parasitol. 18, 885–936.
Landfear, S.M., 2010. Glucose transporters in parasitic protozoa. Methods Mol. Biol. 637, 245–262.
Lane, S., Lloyd, D., 2002. Current trends in research into the waterborne parasite Giardia. Crit. Rev. Microbiol. 28, 123–147.
Lauwaet, T., Smith, A.J., Reiner, D.S., Romijn, E.P., Wong, C.C.L., Davids, B.J., Shah, S. A., Yates, J.R., Gillin, F.D., 2011. Mining the Giardia genome and proteome for conserved and unique basal body proteins. Int. J. Parasitol. 41, 1079–1092.
Leitsch, D., 2015. Drug resistance in the microaerophilic parasite Giardia lamblia. Curr. Trop. Med. Rep. 2, 128–135.
Liao, Y., Smyth, G.K., Shi, W., 2019. The R package Rsubread is easier, faster, cheaper and better for alignment and quantification of RNA sequencing reads. Nucleic Acids Res. 47 e47-e47.
Liu, Y., Beard, W.A., Shock, D.D., Prasad, R., Hou, E.W., Wilson, S.H., 2005. DNA polymerase β and flap endonuclease 1 enzymatic specificities sustain DNA synthesis for long patch base excision repair *. J. Biol. Chem. 280, 3665–3674.
Liu, Y.H., Yuan, S.K., Hu, X.R., Zhang, C.Q., 2019. Shift of sensitivity in botrytis cinerea to benzimidazole fungicides in strawberry greenhouse ascribing to the rising-lowering of E198A subpopulation and its visual, on-site monitoring by loop-mediated isothermal amplification. Sci. Rep. 9, 11644.
Locatelli, C., Pedrosa, R.C., De Bem, A.F., Creczynski-Pasa, T.B., Cordova, C.A., Wilhelm-Filho, D., 2004. A comparative study of albendazole and mebendazole-induced, time-dependent oxidative stress. Redox Rep. 9, 89–95.
Lubega, G.W., Prichard, R.K., 1991. Specific interaction of benzimidazole anthelmintics with tubulin from developing stages of thiabendazole-susceptible and -resistant Haemonchus contortus. Biochem. Pharmacol. 41, 93–101.
Ma'ayeh, S.Y., Liu, J., Peirasmaki, D., Hörnaeus, K., Bergström Lind, S., Grabherr, M., Bergquist, J., Svärd, S.G., 2017. Characterization of the Giardia intestinalis secretome during interaction with human intestinal epithelial cells: the impact on host cells. PLoS Neglected Trop. Dis. 11, e0006120 e0006120.
MacDonald, L.M., Armson, A., Andrew Thompson, R.C., Reynoldson, J.A., 2004. Characterisation of benzimidazole binding with recombinant tubulin from Giardia duodenalis, Encephalitozoon intestinalis, and Cryptosporidium parvum. Mol. Biochem. Parasitol. 138, 89–96.
Machado-Silva, A., Cerqueira, P.G., Grazielle-Silva, V., Gadelha, F.R., Peloso, E.d.F., Teixeira, S.M.R., Machado, C.R., 2016. How Trypanosoma cruzi deals with oxidative

stress: antioxidant defence and DNA repair pathways. Mutat. Res., Rev. Mutat. Res. 767, 8–22.
Manning, G., Reiner, D.S., Lauwaet, T., Dacre, M., Smith, A., Zhai, Y., Svard, S., Gillin, F. D., 2011. The minimal kinome of Giardia lamblia illuminates early kinase evolution and unique parasite biology. Genome Biol. 12, R66.
Martinez-Espinosa, R., Arguello-Garcia, R., Saavedra, E., Ortega-Pierres, G., 2015. Albendazole induces oxidative stress and DNA damage in the parasitic protozoan Giardia duodenalis. Front. Microbiol. 6, 800.
Mirsaeidi, M., Gidfar, S., Vu, A., Schraufnagel, D., 2016. Annexins family: insights into their functions and potential role in pathogenesis of sarcoidosis. J. Transl. Med. 14, 89.
Morrison, H.G., McArthur, A.G., Gillin, F.D., Aley, S.B., Adam, R.D., Olsen, G.J., Best, A. A., Cande, W.Z., Chen, F., Cipriano, M.J., Davids, B.J., Dawson, S.C., Elmendorf, H. G., Hehl, A.B., Holder, M.E., Huse, S.M., Kim, U.U., Lasek-Nesselquist, E., Manning, G., Nigam, A., Nixon, J.E.J., Palm, D., Passamaneck, N.E., Prabhu, A., Reich, C.I., Reiner, D.S., Samuelson, J., Svard, S.G., Sogin, M.L., 2007. Genomic minimalism in the early diverging intestinal parasite Giardia lamblia</ em&gt. Science 317, 1921.
Muller, J., Schildknecht, P., Muller, N., 2013. Metabolism of nitro drugs metronidazole and nitazoxanide in Giardia lamblia: characterization of a novel nitroreductase (GlNR2). J. Antimicrob. Chemother. 68, 1781–1789.
Nosala, C., Hagen, K.D., Dawson, S.C., 2018. 'Disc-o-Fever': getting down with Giardia's groovy microtubule organelle. Trends Cell Biol. 28, 99–112.
Nosala, C., Hagen, K.D., Hilton, N., Chase, T.M., Jones, K., Loudermilk, R., Nguyen, K., Dawson, S.C., 2020. Disc-associated proteins mediate the unusual hyperstability of the ventral disc in Giardia lamblia. J. Cell Sci. 133, jcs227355.
Oxberry, M.E., Thompson, R.C.A., Reynoldson, J.A., 1994. Evaluation of the effects of albendazole and metronidazole on the ultrastructure of Giardia duodenalis, trichomonas vaginalis and Spironucleus muris using transmission electron microscopy. Int. J. Parasitol. 24, 695–703.
Paz-Maldonado, M.T., Arguello-Garcia, R., Cruz-Soto, M., Mendoza-Hernandez, G., Ortega-Pierres, G., 2013. Proteomic and transcriptional analyses of genes differentially expressed in Giardia duodenalis clones resistant to albendazole. Infect. Genet. Evol. 15, 10–17.
Pech-Santiago, E.O., Argüello-García, R., Vázquez, C., Saavedra, E., González-Hernández, I., Jung-Cook, H., Rafferty, S.P., Ortega-Pierres, M.G., 2022. Giardia duodenalis: flavohemoglobin is involved in drug biotransformation and resistance to albendazole. PLoS Pathog. 18, e1010840.
Peirasmaki, D., Ma'ayeh, S.Y., Xu, F., Ferella, M., Campos, S., Liu, J., Svärd, S.G., 2020. High cysteine membrane proteins (HCMPs) are up-regulated during giardia-host cell interactions. Front. Genet. 11.
Prucca, C.G., Slavin, I., Quiroga, R., Elías, E.V., Rivero, F.D., Saura, A., Carranza, P.G., Luján, H.D., 2008. Antigenic variation in Giardia lamblia is regulated by RNA interference. Nature 456, 750–754.
Rescher, U., Gerke, V., 2004. Annexins – unique membrane binding proteins with diverse functions. J. Cell Sci. 117, 2631–2639.
Ritchie, M.E., Phipson, B., Wu, D., Hu, Y., Law, C.W., Shi, W., Smyth, G.K., 2015. Limma powers differential expression analyses for RNA-sequencing and microarray studies. Nucleic Acids Res. 43 e47-e47.
Robertson, L.J., Hanevik, K., Escobedo, A.A., Mørch, K., Langeland, N., 2010. Giardiasis – why do the symptoms sometimes never stop? Trends Parasitol. 26, 75–82.
Robinson, M.D., McCarthy, D.J., Smyth, G.K., 2010. edgeR: a Bioconductor package for differential expression analysis of digital gene expression data. Bioinformatics 26, 139–140.
Rufener, L., Kaminsky, R., Mäser, P., 2009. In vitro selection of Haemonchus contortus for benzimidazole resistance reveals a mutation at amino acid 198 of β-tubulin. Mol. Biochem. Parasitol. 168, 120–122.
Sandhu, H., Mahajan, R.C., Ganguly, N.K., 2004. Flowcytometric assessment of the effect of drugs on Giardia lamblia trophozoites in vitro. Mol. Cell. Biochem. 265, 151–160.
Solaymani-Mohammadi, S., Genkinger, J.M., Loffredo, C.A., Singer, S.M., 2010. A meta-analysis of the effectiveness of albendazole compared with metronidazole as treatments for infections with Giardia duodenalis. PLoS Neglected Trop. Dis. 4, e682.
Steele-Ogus Melissa, C., Johnson Richard, S., MacCoss Michael, J., Paredez Alexander, R., 2021. Identification of actin filament-associated proteins in Giardia lamblia. Microbiol. Spectr. 9, e00558, 00521.
Stenmark, H., 2009. Rab GTPases as coordinators of vesicle traffic. Nat. Rev. Mol. Cell Biol. 10, 513–525.
Torgerson, P.R., Devleesschauwer, B., Praet, N., Speybroeck, N., Willingham, A.L., Kasuga, F., Rokni, M.B., Zhou, X.-N., Fèvre, E.M., Sripa, B., Gargouri, N., Fürst, T., Budke, C.M., Carabin, H., Kirk, M.D., Angulo, F.J., Havelaar, A., de Silva, N., 2015. World Health organization estimates of the global and regional disease burden of 11 foodborne parasitic diseases, 2010: a data synthesis. PLoS Med. 12, e1001920 e1001920.
Tovar, J., León-Avila, G., Sánchez, L.B., Sutak, R., Tachezy, J., van der Giezen, M., Hernández, M., Müller, M., Lucocq, J.M., 2003. Mitochondrial remnant organelles of Giardia function in iron-sulphur protein maturation. Nature 426, 172–176.
Upcroft, J., Mitchell, R., Chen, N., Upcroft, P., 1996. Albendazole resistance in Giardia is correlated with cytoskeletal changes but not with a mutation at amino acid 200 in β-tubulin. Microb. Drug Resist. 2, 303–308.
Vahrmann, A., Šarić, M., Scholze, H., Koebsch, I., 2008. α14-Giardin (annexin E1) is associated with tubulin in trophozoites of Giardia lamblia and forms local slubs in the flagella. Parasitol. Res. 102, 321–326.
Wang, Y., Zhang, H., Gigant, B., Yu, Y., Wu, Y., Chen, X., Lai, Q., Yang, Z., Chen, Q., Yang, J., 2016. Structures of a diverse set of colchicine binding site inhibitors in complex with tubulin provide a rationale for drug discovery. FEBS J. 283, 102–111.
Weiland, M.E.L., McArthur, A.G., Morrison, H.G., Sogin, M.L., Svärd, S.G., 2005. Annexin-like alpha giardins: a new cytoskeletal gene family in Giardia lamblia. Int. J. Parasitol. 35, 617–626.
Wen, L., Lv, G., Zhao, J., Lu, S., Gong, Y., Li, Y., Zheng, H., Chen, B., Gao, H., Tian, C., Wang, J., 2020. In vitro and in vivo effects of artesunate on echinococcus granulosus protoscoleces and metacestodes. Drug Des. Dev. Ther. 14, 4685–4694.
Westermann, S., Weber, K., 2002. Identification of CfNek, a novel member of the NIMA family of cell cycle regulators, as a polypeptide copurifying with tubulin polyglutamylation activity in Crithidia. J. Cell Sci. 115, 5003–5012.
Westermann, S., Weber, K., 2003. Post-translational modifications regulate microtubule function. Nat. Rev. Mol. Cell Biol. 4, 938–948.
Woessner, D.J., Dawson, S.C., 2012. The Giardia median body protein is a ventral disc protein that is critical for maintaining a domed disc conformation during attachment. Eukaryot. Cell 11, 292–301.
Wu, D., Lim, E., Vaillant, F., Asselin-Labat, M.L., Visvader, J.E., Smyth, G.K., 2010. ROAST: rotation gene set tests for complex microarray experiments. Bioinformatics 26, 2176–2182.
Xie, N., Zhang, L., Gao, W., Huang, C., Huber, P.E., Zhou, X., Li, C., Shen, G., Zou, B., 2020. NAD+ metabolism: pathophysiologic mechanisms and therapeutic potential. Signal Transduct. Targeted Ther. 5, 227.
Xu, F., Jex, A., Svärd, S.G., 2020. A chromosome-scale reference genome for Giardia intestinalis WB. Sci. Data 7, 38.
Xu, Y., Qing, W., Wang, Z., Chen, L., Wang, L., Lv, H., Jiang, Y., 2022. In vitro protoscolicidal effects of lithocholic acid on protoscoleces of Echinococcus granulosus and its mechanism. Exp. Parasitol. 239, 108280.
Yarden, O., Katan, T., 1993. Mutations leading to substitutions at amino acids 198 and 200 of beta-tubulin that correlate with benomyl-resistance phenotypes of field strains of Botrytis cinerea. Phytopathology 83, 1478–1483.